

The Fatty Acid Biosynthesis Enzyme FabI Plays a Key Role in the Development of Liver-Stage Malarial Parasites

Min Yu,^{1,2,16} T. R. Santha Kumar,^{1,2,16} Louis J. Nkrumah,² Alida Coppi,³ Silke Retzlaff,⁴ Celeste D. Li,¹ Brendan J. Kelly,⁵ Pedro A. Moura,¹ Viswanathan Lakshmanan,^{2,14} Joel S. Freundlich,⁶ Juan-Carlos Valderramos,¹ Catherine Vilcheze,² Mark Siedner,⁵ Jennifer H.-C. Tsai,⁶ Brie Falkard,¹ Amar bir Singh Sidhu,¹ Lisa A. Purcell,^{1,15} Paul Gratraud,⁷ Laurent Kremer,^{7,8} Andrew P. Waters,⁹ Guy Schiehser,¹⁰ David P. Jacobus,¹⁰ Chris J. Janse,¹¹ Arba Ager,¹² William R. Jacobs, Jr.,^{2,13} James C. Sacchetti,⁶ Volker Heussler,⁴ Photini Sinnis,³ and David A. Fidock^{1,5,*}

¹Department of Microbiology, Columbia University, New York, NY 10032, USA

²Department of Microbiology and Immunology, Albert Einstein College of Medicine, Bronx, NY 10461, USA

³Department of Medical Parasitology, New York University School of Medicine, New York, NY 10010, USA

⁴Bernhard Nocht Institute for Tropical Medicine, Hamburg, Germany

⁵Department of Medicine, Columbia University, New York, NY 10032, USA

⁶Department of Biochemistry and Biophysics, Texas A&M University, College Station, TX 77843, USA

⁷Universités de Montpellier II and I, CNRS UMR5235, Montpellier, France

⁸INSERM, DIMNP, Montpellier, France

⁹Wellcome Centre for Molecular Parasitology, University of Glasgow, Scotland, UK

¹⁰Jacobus Pharmaceutical Company, Princeton, NJ 08540, USA

¹¹Department of Parasitology, Centre of Infectious Diseases, Leiden University, The Netherlands

¹²Department of Microbiology and Immunology, University of Miami, Miami, FL 33177, USA

¹³Howard Hughes Medical Institute, Albert Einstein College of Medicine, Bronx, NY 10461, USA

¹⁴Present address: Department of Molecular Biology, Princeton University, Princeton, NJ 08544, USA

¹⁵Present address: Regeneron, Tarrytown, NY 10591, USA

¹⁶These authors contributed equally to this work

*Correspondence: df2260@columbia.edu

DOI 10.1016/j.chom.2008.11.001

SUMMARY

The fatty acid synthesis type II pathway has received considerable interest as a candidate therapeutic target in *Plasmodium falciparum* asexual blood-stage infections. This apicoplast-resident pathway, distinct from the mammalian type I process, includes FabI. Here, we report synthetic chemistry and transfection studies concluding that *Plasmodium* FabI is not the target of the antimalarial activity of triclosan, an inhibitor of bacterial FabI. Disruption of *fabI* in *P. falciparum* or the rodent parasite *P. berghei* does not impede blood-stage growth. In contrast, mosquito-derived, FabI-deficient *P. berghei* sporozoites are markedly less infective for mice and typically fail to complete liver-stage development in vitro. This defect is characterized by an inability to form intrahepatic merosomes that normally initiate blood-stage infections. These data illuminate key differences between liver- and blood-stage parasites in their requirements for host versus de novo synthesized fatty acids, and create new prospects for stage-specific antimalarial interventions.

INTRODUCTION

Plasmodium parasites must coordinate the salvage of host factors with *de novo* biosynthesis pathways in order to meet

the unique demands of each intracellular stage of their life cycle. In mammals, this begins with the bite of an infected *Anopheles* mosquito. The intradermally injected sporozoites (SPZs) then migrate to the liver and invade hepatocytes (Amino et al., 2008). Liver-stage development involves the transformation of an intracellular sporozoite, bounded by an inner parasite plasma membrane (PPM) and an outer parasitophorous vacuolar membrane (PVM), into a liver-stage trophozoite. This stage undergoes prolific nuclear division and membrane synthesis with commensurate metabolic demands. In the case of *P. falciparum*, the most lethal etiologic agent of human malaria, each infected hepatocyte produces up to 10,000–30,000 merozoites, contained within an intrahepatic merosome, over 6–7 days.

Liberated liver-stage merozoites enter the bloodstream, where they invade red blood cells (RBCs) and initiate the asexual blood stages that cause clinical manifestations of disease. Parasite development inside these anucleate cells displays several fundamental differences from the liver stages (Silvie et al., 2008b). These include the ability of asexual blood-stage parasites to degrade hemoglobin and detoxify heme (processes that are key to the mode of action of multiple antimalarials), and also to modify the host cell membrane, such that the infected RBCs can sequester in the microvasculature. The entire asexual cycle is completed within 48 hr, producing 8–24 infectious merozoites per infected RBC. In contrast to the small liver-stage inoculum, numbers of infected RBCs can exceed 10^{12} per host (Greenwood et al., 2008). Intraerythrocytic parasites can also transform into sexual gametocyte stages. Upon their ingestion by a feeding *Anopheles* mosquito, these parasites undergo fertilization and

sexual recombination, ultimately producing oocyst SPZs that migrate to the salivary glands, ready to initiate a new round of infection.

The prodigious proliferative capacity of malarial parasites necessitates access to an abundant source of fatty acids (FAs). These carboxylic acid-linked acyl chains are required for the production of lipid species that are essential for parasite membrane and lipid body biogenesis (Palacpac et al., 2004). FAs are also required for glycosylphosphatidylinositol (GPI) moieties that serve to anchor parasite membrane proteins (Gilson et al., 2006). FA and phospholipid concentrations are, respectively, 6-fold and 3- to 5-fold higher in infected compared to uninfected RBCs. This was initially attributed to FA salvage from host plasma, as parasites were thought to be incapable of de novo synthesis (Vial and Ancelin, 1992). The paradigm changed with the discovery that *P. falciparum* harbors components of a type II FA biosynthesis (FAS-II) pathway (Ralph et al., 2004). A subsequent study reported that *P. falciparum* asexual blood stages had FAS-II activity, producing FAs with chain lengths of C₁₀–C₁₄ (Surolia and Surolia, 2001). FAS-II enzymes have been localized to the apicoplast, a nonphotosynthetic plastid organelle of cyanobacterial origin. In addition to FA biosynthesis, the apicoplast harbors unique pathways for the synthesis of isoprenoids and heme and shares lipoic acid synthesis and salvage pathways with the mitochondria. The discovery that antibiotics with antimalarial activity inhibit apicoplast function has highlighted the therapeutic potential of targeting this organelle (Ralph et al., 2004).

The FAS-II pathway in *Plasmodium* has been of particular therapeutic interest, because it is distinct from the type I (FAS-I) pathway found in mammals. FAS-II requires acetyl-Coenzyme A (CoA), which can be converted from pyruvate by the pyruvate dehydrogenase complex. Acetyl-CoA carboxylase converts acetyl-CoA to malonyl-CoA, which is tethered to an acyl carrier protein (ACP) by malonyl-CoA:ACP transacylase (FabD). This produces malonyl-ACP, which, in conjunction with acetyl-CoA, is acted upon by β -ketoacyl-ACP synthase III (Fab H) to form β -ketoacyl-ACP. This precursor enters the FAS-II elongation cycle, mediated by FabB/F (β -ketoacyl-acyl-carrier-protein (ACP) synthase), FabG (β -ketoacyl-ACP reductase), FabZ/A (β -hydroxyacyl-ACP dehydratase), and FabI (*trans*-2-enoyl-ACP reductase). These four FAS-II enzymes iteratively catalyze the addition of two carbon chains to a growing fatty acyl carbon chain via condensation, reduction, dehydration, and reduction steps, respectively. In contrast, FAS-I contains all four enzymatic functionalities within a single, large polypeptide (Mazumdar and Striepen, 2007).

Studies from pathogenic bacteria have confirmed the therapeutic value of FAS-II inhibitors (Zhang et al., 2006). These include triclosan, a microbicide widely used in consumer products. A highly cited report describing triclosan antimalarial activity in vitro against *P. falciparum* and in vivo against the rodent parasite *P. berghei*, directed against the pathogenic asexual blood stages, generated tremendous interest in this compound and its predicted target, FabI (Surolia and Surolia, 2001). This led to the structural elucidation of the *P. falciparum* FabI (PfFabI; PlasmoDB gene ID PFF0730c) homotetramer, to which triclosan: NAD⁺ adducts bind in the active site, and propelled structure-guided efforts to develop novel antimalarials based on triclosan (Freundlich et al., 2007; Muralidharan et al., 2003; Perozzo

et al., 2002). Here, we report our investigations into a series of analogs designed to improve on the antimalarial properties of triclosan and our ensuing studies that focused on the biological role of FabI.

RESULTS

Triclosan Activity against *Plasmodium* Asexual Blood Stages Does Not Correlate with Its Inhibition of Purified Recombinant FabI

We initiated a structure-guided medicinal chemistry program to improve the potency of triclosan by modifying substituents around its diaryl ether scaffold. This led us to synthesize 80 analogs (Figure 1A), for which only a single position was modified to reduce the likelihood of creating off-target activity. These analogs, grouped by the carbon position that was modified (see Figure 1B inset; detailed in Table S1 in the Supplemental Data), were evaluated for their inhibition of cultured *P. falciparum* asexual blood-stage parasites (3D7 and Dd2 lines), and separately for inhibition of purified PfFabI enzyme. Activities were compared against triclosan, which yielded mean IC₅₀ values of 1.8 and 2.1 μ M against the 3D7 and Dd2 lines and an EC₅₀ value of 73 nM against purified PfFabI. Individual analog series showed substantial differences in their inhibitory activities (Figure 1A). The 2'-position analog series afforded the most potent inhibitors in the parasite assays, yet showed minimal inhibition of PfFabI. Modifications at the 4'- or 5-position afforded a few modest improvements in efficacy, mostly against PfFabI, whereas changes at the 4- or 6-position generally produced less potent inhibitors. We also noted that compound series with similar mean potencies against PfFabI (e.g., the 4'- and 5-position analogs) exhibited nearly 10-fold differences in their mean antiparasitic activities. Further analysis revealed a lack of a significant association between enzyme and parasite inhibition, as evidenced by the Pearson r^2 values of 0.13 and 0.15 obtained by plotting these data for 3D7 and Dd2, respectively (Figure 1B; data not shown). While chemical properties such as membrane permeability and solubility might obscure close whole-cell and enzyme correlations for on-target compounds, our data nonetheless raised doubts that triclosan analogs acted against asexual blood-stage parasites by inhibiting PfFabI.

In parallel with these studies, we re-evaluated the in vivo efficacy of triclosan. A previous report had documented that 4 days of subcutaneous injections of triclosan at 3 mg/kg/day could suppress *P. berghei* parasitemia by 75%, and that injections with doses of 38 mg/kg/day cured the infected mice with 100% efficacy (Surolia and Surolia, 2001). We tested both per oral (PO) and subcutaneous (SC) routes of triclosan, administered over a range of 16–512 mg/kg/day for 3 days with a twice daily divided dose, to mice infected 3 days prior with *P. berghei* (KBG-173 line). Parasitemias were recorded on day 6 postinfection (i.e., 1 day after the last dose of triclosan) and were 61% or 57% (for PO or SC, respectively) in control (infected and placebo-treated) mice. Increasing the triclosan concentrations from 16 to 128 mg/kg/day caused a dose-dependent decrease in parasitemias, to a minimum of 27% or 13% with 128 mg/kg/day triclosan administered PO or SC, respectively (Figure 1C). Higher doses failed to further suppress the parasitemias.

Assessment of survival showed that all control mice died by days 10 (PO) or 12 (SC) (Figures 1D and 1E). Oral administration

Cell Host & Microbe

A Key Role for FabI in Plasmodium Liver Stages

A Activity of triclosan analogs on *Plasmodium falciparum* cultures and purified PfFabI

Series	Number of Compounds	<i>P. falciparum</i> 3D7 (μM)	<i>P. falciparum</i> Dd2 (μM)	Purified PfFabI (nM)
		Median (min, max)	Median (min, max)	Median (min, max)
Triclosan	1	2.8	3.8	73
2'-Position Analogs	15	0.4 (0.1, 14)	0.4 (0.1, 17)	18000 (3300, 35000)
4'-Position Analogs	24	44 (2.1, 120)	49 (3.2, 110)	315 (57, 3000)
4-Position Analogs	4	16 (1.9, 91)	16 (2.6, 54)	3290 (280, 6300)
5-Position Analogs	25	5.6 (1.6, 40)	7.2 (2.5, 45)	290 (38, 33000)
6-Position Analogs	12	2.9 (1.5, 47)	2.4 (1.2, 41)	830 (180, 2900)

Values represent the concentration that produced either 50% inhibition of *P. falciparum* growth (IC_{50}) or purified PfFabI enzymatic activity (EC_{50}). In comparison, chloroquine produced mean IC_{50} values of 30 nM and 280 nM against 3D7 and Dd2 parasites, respectively.

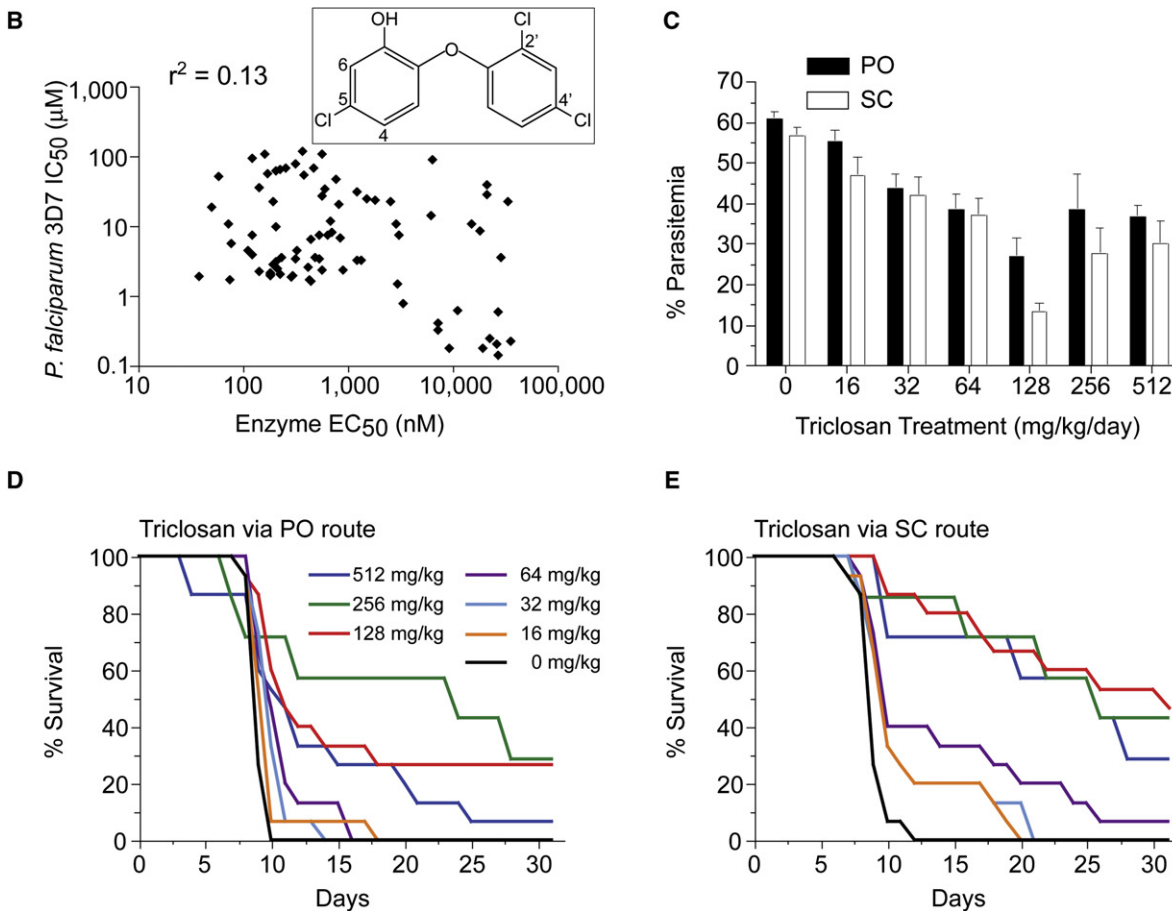


Figure 1. Triclosan Displays In Vitro Activity against *P. falciparum* that Does Not Correlate with Inhibition of FabI and Is Less Effective in Curing Rodent Malaria Than Previously Reported

(A) Inhibitory activity of subclasses of triclosan analogs against *P. falciparum* lines and purified PfFabI enzyme.
 (B) Log scale scatter plot of the activity of triclosan and its analogs against *P. falciparum* 3D7 parasites and purified PfFabI, showing the Pearson r^2 goodness of fit value. The inset shows triclosan (5-chloro-2-(2,4-dichlorophenoxy)phenol) with carbon atoms numbered where substitutions were made.
 (C) Percent parasitemias plotted for the groups of mice receiving varying doses of triclosan, administered either PO or SC twice daily for 3 days. Mean values (\pm SEM) were calculated from groups of 7–8 mice tested on two separate occasions.
 (D and E) Kaplan-Meier survival curves for the groups receiving daily triclosan doses as indicated.

of 64 mg/kg/day triclosan yielded a slight extension in survival times, and doses of 128 or 256 mg/kg/day produced 30% survival rates measured at day 31. Increasing the dose to 512 mg/kg/day led to some early mortality and decreased overall survival rates,

suggesting some toxicity. Via the SC route, triclosan was moderately more effective, although survival never exceeded 50%. In vivo tests with several analogs (compounds 18, 20, 22, 41, 45, and 60 in Table S1), whose in vitro potencies were comparable

Table 1. Recombinant and Wild-Type Parasite Lines Used in This Study

Parasite line	Species	Recombinant	Transfection plasmid	Endogenous <i>fabI</i> gene present	Selectable marker gene ^a	Comment
Pf <i>fabI</i> (A217V) ^{Dd2}	<i>P. falciparum</i>	Yes	<i>pfabi</i> (A217V)-V5-attP	Yes	<i>bsd</i> , <i>hdhfr</i>	[1]
Pf <i>fabI</i> (WT) ^{Dd2}	<i>P. falciparum</i>	Yes	<i>pfabi</i> (WT)-V5-attP	Yes	<i>bsd</i> , <i>hdhfr</i>	[2]
Dd2 ^{attB}	<i>P. falciparum</i>	Yes	None	Yes	<i>hdhfr</i>	[3]
Dd2	<i>P. falciparum</i>	No	None	Yes	None	[4]
Pf <i>fabI</i> (A217V) ^{3D7}	<i>P. falciparum</i>	Yes	<i>pfabi</i> (A217V)-V5-attP	Yes	<i>bsd</i> , <i>hdhfr</i>	[1]
Pf <i>fabI</i> (WT) ^{3D7}	<i>P. falciparum</i>	Yes	<i>pfabi</i> (WT)-V5-attP	Yes	<i>bsd</i> , <i>hdhfr</i>	[2]
3D7 ^{attB}	<i>P. falciparum</i>	Yes	None	Yes	<i>hdhfr</i>	[3]
3D7	<i>P. falciparum</i>	No	None	Yes	None	[4]
PfΔ <i>fabI</i> ¹	<i>P. falciparum</i>	Yes	<i>pcam-bsd-Δpfabi</i>	No	<i>bsd</i>	[5]
PfΔ <i>fabI</i> ²	<i>P. falciparum</i>	Yes	<i>pcam-bsd-Δpfabi</i>	No	<i>bsd</i>	[5]
PbΔ <i>fabI</i>	<i>P. berghei</i>	Yes	<i>pLitmus28-Δpbfabi</i>	No	<i>Tgdhfr-ts</i>	[6]
Pb <i>fabI</i> ^{Rec}	<i>P. berghei</i>	Yes	<i>pLitmus28-pbfabi</i> ^{Rec}	Yes (reinserted)	<i>Tgdhfr-ts</i>	[7]
ANKA	<i>P. berghei</i>	No	None	Yes	None	[4]

[1]: Expresses mutant *pfabi*(A217V)-V5 transgene from *calmodulin* promoter, integrated into *cg6* attB site.

[2]: Expresses wild type *pfabi*(WT)-V5 transgene from *calmodulin* promoter, integrated into *cg6* attB site.

[3]: Contains attB site integrated into *cg6* locus. Parental line for transfection with attP-containing *pfabi* transgene constructs.

[4]: Wild-type nonrecombinant line.

[5]: Endogenous *pfabi* locus disrupted by single cross-over homologous recombination, clones 1 and 2.

[6]: Endogenous *pbfabi* locus deleted by double cross-over homologous recombination.

[7]: Endogenous *pbfabi* locus replaced with a wild type copy of *pbfabi* plus the *Tgdhfr-ts* selection cassette.

^a Selection was performed using blasticidin hydrochloride for *bsd*, WR99210 for *hdhfr*, and pyrimethamine for *Tgdhfr-ts*.

to triclosan, revealed no improvements over the parent compound (A.A. and D.P.J., unpublished data). We concluded that, under our experimental conditions, triclosan had reduced anti-malarial potency in vivo as compared to the earlier report (Surolia and Surolia, 2001). Furthermore, the in vitro potency of triclosan analogs did not correlate with their inhibition of FabI enzymatic activity.

Transgene Expression of a Mutant FabI that Is Biochemically Resistant to Triclosan Does Not Decrease *P. falciparum* Susceptibility to this Agent

To further investigate the role of FabI in the mode of action of triclosan, we transfected *P. falciparum* asexual blood-stage parasites with plasmids expressing V5 epitope-tagged forms of *pfabi* that were either wild-type (WT) or that encoded the A217V mutation. This mutation was selected because it confers a 7000-fold decrease in triclosan binding affinity for recombinant PfFabI (Kapoor et al., 2004). To express these *pfabi* transgenes, we selected the *calmodulin* (PF14_0323) promoter, which is highly active in asexual blood stages (<http://www.PlasmoDB.org>). Integration of these plasmids (named *pfabi*(A217V)-V5-attP and *pfabi*(WT)-V5-attP) (Table 1) into the *P. falciparum* genome was achieved using the Bxb1 serine integrase-mediated attB × attP system of recombination, which delivers transgenes into the attB-marked *cg6* locus and results in a genetically and phenotypically homogeneous population of recombinant parasite lines (Nkrumah et al., 2006). The transfections, performed with Dd2^{attB} and 3D7^{attB} parasites, produced the transgenic lines Pf*fabI*(A217V)^{Dd2}, Pf*fabI*(WT)^{Dd2}, Pf*fabI*(A217V)^{3D7}, and Pf*fabI*(WT)^{3D7} (Table 1 and Figure S1A). Southern blot analysis confirmed correct integration of the *pfabi* transgenic copies into the *cg6*-attB site and the predicted organization of the endogenous *pfabi* locus (Figure S1B; data not shown). Western

blot analysis with anti-V5 antibodies revealed the expression of ~46 kDa V5-tagged PfFabI proteins in all four lines (Figure S1C). Immunofluorescence assays with the Pf*fabI*(A217V)^{Dd2} line showed colocalization of PfFabI-V5 and the apicoplast-resident ACP in a compartment distinct from the nucleus (stained with Hoechst 33342) and the mitochondrion (stained with MitoTracker Red), thus confirming trafficking of V5-tagged PfFabI to the apicoplast (Figures 2A and 2B). We proceeded to measure the triclosan susceptibility of our transgenic and parental lines. Results from drug susceptibility assays showed no significant difference in either IC₅₀ or IC₉₀ values between recombinant lines expressing mutant or WT PfFabI (Figure 2C; values provided in legend).

P. falciparum FabI Is Not Expressed at Detectable Levels in Asexual Blood-Stage Parasites

Subsequent northern blot experiments detected the presence of *pfabi* transcripts only in the transgenic lines (Pf*fabI*(A217V)^{Dd2}, Pf*fabI*(WT)^{Dd2}, Pf*fabI*(A217V)^{3D7}, and Pf*fabI*(WT)^{3D7}) that express an additional *pfabi* copy from the highly active mature-stage *calmodulin* promoter, and not in the lines expressing endogenous *pfabi* alone (Dd2^{attB}, Dd2, 3D7^{attB}, and 3D7) (Figure 2D). We attribute the apparent increase in *pfabi* transcripts in the Pf*fabI*(A217V)^{Dd2} and Pf*fabI*(A217V)^{3D7} lines, compared to the Pf*fabI*(WT)^{Dd2} and Pf*fabI*(WT)^{3D7} lines, to the higher proportions of mature-stage parasites in the former at the time of RNA harvest. To confirm the lack of endogenous *pfabi* expression at the protein level, we raised rabbit polyclonal antiserum against purified recombinant PfFabI. Western blot analysis with extracts of parasites expressing *calmodulin* promoter-driven PfFabI-V5 showed that the antiserum and monoclonal antibodies against the V5 epitope tag both detected a ~46 kDa protein (Figure 2E). The anti-PfFabI antiserum did not detect any protein in extracts

Cell Host & Microbe

A Key Role for FabI in Plasmodium Liver Stages

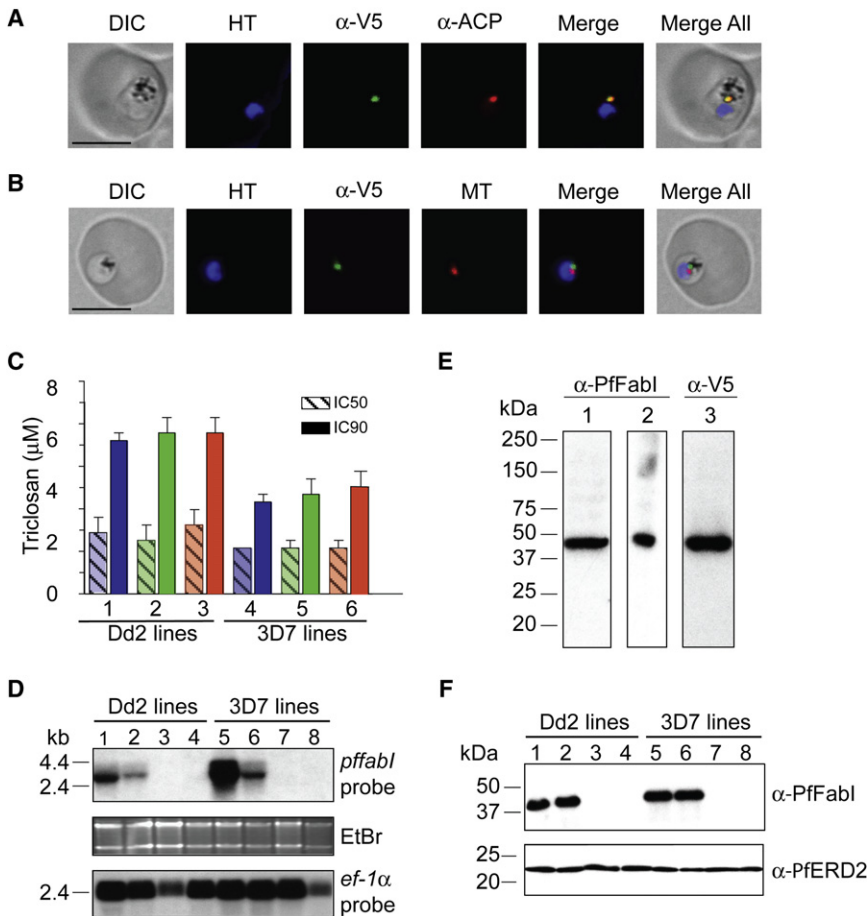


Figure 2. Transgenic Expression of Mutant *pffabl* Does Not Confer Triclosan Resistance In Vitro

(A and B) Fluorescence microscopy of *Pffabl*(A217V)^{Dd2} parasites. Proper targeting of *Pffabl*-V5 to the apicoplast was illustrated by colocalization of the V5 epitope tag of the mutant protein and ACP. This signal was adjacent to the mitochondrion that was visualized using MitoTracker Red (MT). Scale bar is 5 μm. DIC, differential interference contrast; HT, Hoechst 33342 nuclear dye; α-V5 and α-ACP, antibodies to V5 and ACP. Similar results were obtained with *Pffabl*(WT)^{Dd2} (data not shown) and with an earlier transgenic Dd2 line that expressed GFP-tagged *PfFabI* from the same *calmodulin* promoter (Nkrumah et al., 2006).

(C) Inhibitory activity of triclosan against *P. falciparum* lines expressing either mutant or WT *PfFabI*. Data were derived from three separate experiments performed in duplicate. Lanes (with mean ± SEM). IC₅₀, IC₉₀ values in μM) 1: *Pffabl*(A217V)^{Dd2} (2.8 ± 0.7, 6.9 ± 0.4); 2: *Pffabl*(WT)^{Dd2} (2.5 ± 0.7; 7.3 ± 0.7); 3: Dd2^{attB} (3.1 ± 0.7, 7.2 ± 0.7); 4: *Pffabl*(A217V)^{3D7} (2.1 ± 0.4, 4.2 ± 0.3); 5: *Pffabl*(WT)^{3D7} (2.0 ± 0.3, 4.5 ± 0.7); 6: 3D7^{attB} (2.1 ± 0.2, 4.8 ± 0.6). (D) Northern blot analysis showing presence of *pffabl* transcripts only in the lines expressing this transgene from the *calmodulin* promoter. EtBr, ethidium bromide. Lanes 1: *Pffabl*(A217V)^{Dd2}; 2: *Pffabl*(WT)^{Dd2}; 3: Dd2^{attB}; 4: Dd2; 5: *Pffabl*(A217V)^{3D7}; 6: *Pffabl*(WT)^{3D7}; 7: 3D7^{attB}; 8: 3D7. *ef-1α* was used as a loading control.

(E) Evidence that α-*PfFabI* and α-V5 antibodies recognize the same protein in asexual blood-stage parasites expressing *calmodulin* promoter-driven *PfFabI*. Lanes 1 and 3: *Pffabl*(A217V)^{Dd2}; 2: *Pffabl*(WT)^{Dd2} (these lines express *PfFabI* with a V5 epitope).

(F) Western blot analysis showing the detection of *PfFabI* only in the lines expressing *pffabl* transgenes from the *calmodulin* promoter. α-*PfERD2* antibodies were used as a loading control. Lanes 1–8 are the same as in (D).

of control parasites expressing *pffabl* from its endogenous promoter (Figure 2F).

FabI Is Not Required for Normal Propagation of *P. falciparum* Asexual Blood-Stage Parasites, and Its Absence Does Not Alter Parasite Susceptibility to Triclosan

These findings led us to question whether *pffabl* is required for *P. falciparum* asexual blood-stage growth in vitro. To test this, we designed a DNA construct (*pcam-bsd-Δpffabl*), which contained an internal region of the *pffabl* coding sequence (encoding amino acids 98–295) such that homologous recombination between this fragment and the endogenous *pffabl* gene would separate the full-length sequence into two truncated fragments (Figure S2A). The upstream fragment lacked the 3' end of the gene corresponding to amino acids 296–432 (thereby eliminating the α6–α9 helices and β6–β7 strands that contribute to forming the NADH-binding Rossmann fold). The downstream fragment lacked a promoter and the first 98 amino acids that included the bipartite targeting sequence predicted to be required for protein trafficking to the apicoplast (Perozzo et al., 2002). Transfection of cultured

Dd2 parasites with this knockout construct resulted in the generation of parasite clones (*PfΔfabI*¹ and *PfΔfabI*²), in which the *pffabl* gene had been disrupted by single site crossover and plasmid integration, as confirmed by PCR and Southern blot analyses (Table 1 and Figures S2B and S2C). Measurements of parasitemia over a 2-month period revealed equivalent growth rates (averaging 5.0- to 5.6-fold multiplication per 48 hr cycle of RBC invasion, intracellular development, and egress) between these knockout clones and parental Dd2. These data demonstrated the nonessentiality of *pffabl* for asexual blood-stage propagation, and implied that the activity of triclosan against these stages could not result from inhibition of *PfFabI*. This was confirmed with drug susceptibility assays that revealed similar triclosan susceptibilities in *PfΔfabI*¹, *PfΔfabI*², and the parental Dd2 line (mean ± SEM; IC₅₀ values of 2.2 ± 0.2, 2.4 ± 0.3, and 2.1 ± 0.3 μM, respectively, derived from three separate experiments performed in duplicate).

Deletion of *P. berghei fabI*, the *pffabl* Ortholog, Does Not Affect Propagation of Blood-Stage Parasites In Vivo

Our *P. falciparum* in vitro data led us to examine whether this protein was essential for proliferation of asexual blood stages

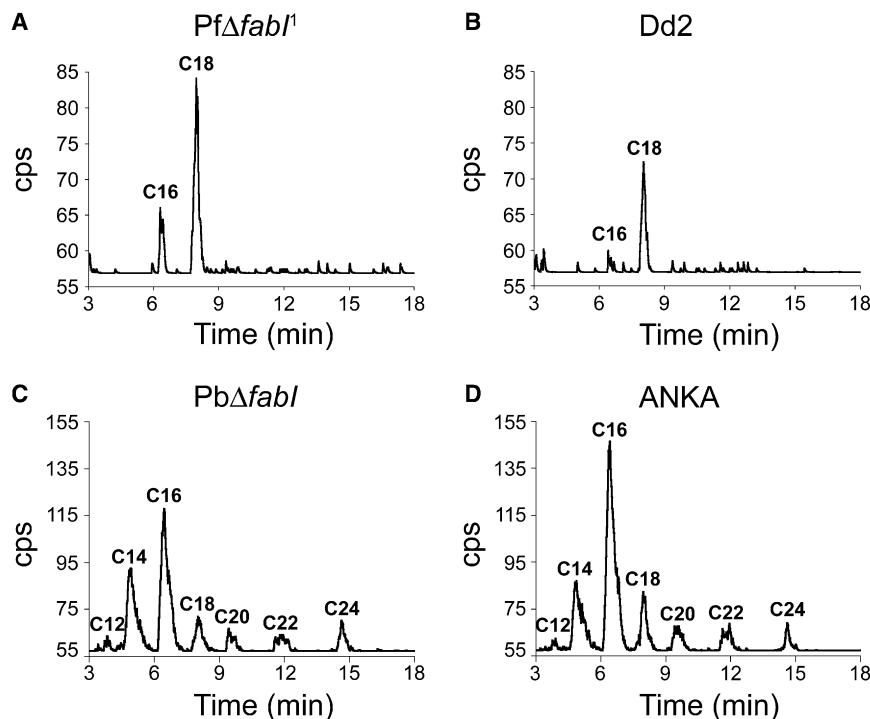


Figure 3. Plasmodium Asexual Blood-Stage Parasites Modify FAs in the Absence of FabI (A–D) HPLC analysis of extractable FA *p*-bromophenylacetyl esters from *in vitro* cultures of the *P. falciparum* lines PfΔfabI¹ (A) and Dd2 (B), or *ex vivo* cultures of the *P. berghei* lines PbΔfabI (C) and ANKA (D). Acyl chain lengths are indicated. CPS, counts per second.

in vivo. For this, we used the highly virulent *P. berghei* ANKA rodent malaria model. Comparisons of the amino acid sequences of PfFabI and its predicted ortholog in *P. berghei*, PbFabI (PB000088.02.0), revealed 62% identity and 74% similarity (Figure S3A). Bacterial expression and purification of PbFabI enabled us to elucidate its structure at 2.5 Å resolution. Superimposing this with the known PfFabI structure (Perozzo et al., 2002) revealed a nearly identical organization with each subunit in the tetramer containing nine α helices and seven β sheets (Figure S3B). Detailed inspection of the active sites revealed these to be indistinguishable (Figure S3C). From these studies, we can confidently predict that PbFabI and PfFabI fulfill the same enzymatic function for *Plasmodium* parasites.

We transfected *P. berghei* ANKA parasites with a DNA construct termed pLitmus28-Δ*pbfabI*. This was designed to permit double crossover, resulting in complete deletion of the endogenous *pbfabI* locus and its replacement by the *T. gondii* dihydrofolate reductase-thymidylate synthase (*Tgdhfr-ts*) selectable marker that confers resistance to pyrimethamine. From this transfection, we selected mutant parasites and used limiting dilution to obtain a clone, termed PbΔ*fabI* (Table 1). PCR and Southern blot analyses confirmed correct integration of the DNA construct and deletion of the *pbfabI* coding sequence in this clone (Figures S4A–S4D). As a “knockin” control, we utilized a similar double crossover strategy to replace the endogenous gene with a construct that reinserted a full-length, functional *pbfabI* gene under control of the endogenous promoter, as well as the *Tgdhfr-ts* selectable marker. This yielded the Pb*fabI*^{Rec} clone, whose recombinant locus was confirmed by PCR and Southern blot hybridization (Figures S4B–S4D). Measurements of parasitemia in mice infected with PbΔ*fabI*, Pb*fabI*^{Rec}, or paren-

tal ANKA revealed similar rates of proliferation, calculated to be 4.8 ± 1.4 , 5.5 ± 2.2 , and 4.4 ± 1.7 per 24 hr cycle, respectively, in two comparative experiments with groups of four mice each (values represents means \pm SD; Figure S4E). These values were not statistically different between lines, as determined by Mann-Whitney tests. Thus, there was no substantial decrease in asexual blood-stage *in vivo* viability upon deletion of *pbfabI*.

Drug susceptibility assays with *P. berghei* asexual blood stages tested *ex vivo* showed equivalent triclosan IC₅₀ values in the PbΔ*fabI*, Pb*fabI*^{Rec}, and ANKA lines (means \pm SEM of 1.4 ± 0.1 , 1.5 ± 0.2 , and 1.2 ± 0.1 μ M, respectively). Control as-

says with the unrelated antimalarial chloroquine produced IC₅₀ values of 11.0 ± 0.1 , 13.0 ± 0.6 , and 10.4 ± 0.3 nM in these lines, respectively. These results, combined with the *P. falciparum* studies, conclusively demonstrate that the blood-stage activity of triclosan is not attributable to inhibition of FabI.

Plasmodium Asexual Blood-Stage Parasites Lacking FabI Can Produce FA Species

The availability of parasite lines lacking FabI allowed us to determine whether *Plasmodium* asexual blood stages utilize the FAS-II pathway to synthesize FAs *de novo*. We incubated synchronized trophozoite-stage *P. falciparum* and *P. berghei* control and *fabI* knockout parasites with [¹⁴C]-acetate, a radiolabeled FA precursor, then extracted the free FAs that had incorporated this substrate and analyzed them by reversed-phase high performance liquid chromatography (HPLC). In *P. falciparum*, this led us to detect radiolabeled C₁₆ and C₁₈ FAs in both the PfΔ*fabI*¹ and Dd2 lines (Figures 3A and 3B). Thus, extension of FAs could occur in the absence of the key FAS-II enzyme FabI. In a separate experiment, we incubated PfΔ*fabI*¹ and other *P. falciparum* lines with [¹⁴C]-acetate, extracted their FAs, and analyzed them by reversed-phase thin layer chromatography. This confirmed the production of radiolabeled C₁₆ and C₁₈ independently of FabI (Figure S2D). We note that these findings are in contrast with an earlier report that *P. falciparum* asexual blood-stage parasites synthesize C₁₀–C₁₄ FAs (Surolia and Surolia, 2001).

[¹⁴C]-acetate incorporation studies with the *P. berghei* lines produced evidence of *de novo* FA elongation with PbΔ*fabI* parasites, with no visible difference between the PbΔ*fabI* and parental ANKA lines in terms of the lengths of FAs that were produced (Figures 3C and 3D). In contrast to *P. falciparum*, the rodent parasites synthesized FA chain lengths of C₁₂–C₂₄. No radiolabeled FAs

Cell Host & Microbe

A Key Role for FabI in Plasmodium Liver Stages

Table 2. *PbΔfabI* Sporozoites Are Highly Attenuated in Their Infectivity for the Host

Experiment	Parasites	Route	Sporozoites	Number of infected mice	Prepatent period (day) ^a
1	ANKA	Intravenous	1,000	5 of 5	4.8
	<i>PbfabI</i> ^{Rec}	Intravenous	1,000	5 of 5	4.6
	<i>PbΔfabI</i>	Intravenous	1,000	2 of 5	8.5
	<i>PbΔfabI</i>	Intravenous	10,000	5 of 5	8.0
2	ANKA	Intravenous	1,000	6 of 6	3.7
	<i>PbfabI</i> ^{Rec}	Intravenous	1,000	5 of 5	4.0
	<i>PbΔfabI</i>	Intravenous	1,000	1 of 6	8.0
	<i>PbΔfabI</i>	Intravenous	10,000	5 of 5	7.8
3	ANKA	Intravenous	1,000	5 of 5	3.8
	<i>PbfabI</i> ^{Rec}	Intravenous	1,000	5 of 5	4.0
	<i>PbΔfabI</i>	Intravenous	1,000	2 of 5	8.5
	<i>PbΔfabI</i>	Intravenous	10,000	3 of 5	8.3
4	ANKA	Mosquito bite	From 20 mosquitoes	5 of 5	4.0
	<i>PbfabI</i> ^{Rec}	Mosquito bite	From 20 mosquitoes	5 of 5	4.0
	<i>PbΔfabI</i>	Mosquito bite	From 20 mosquitoes	4 of 5	9.3

^a Represents mean number of days after sporozoite inoculation until microscopic detection of blood stage parasites. Mice were examined for blood stage infections daily until day 28. Means were calculated only from the mice that developed a patent infection.

were observed with rodent or human uninfected RBC controls (data not shown). These data provide evidence that the two *Plasmodium* species differ in the range of FAs that they can extend de novo, yet they share the common characteristic that FabI is not required.

***P. berghei* SPZs Lacking FabI Are Markedly Attenuated in Their Ability to Progress to Asexual Blood-Stage Infections**

The availability of a *P. berghei* line (*PbΔfabI*) lacking FabI made it possible to explore the role of this protein in other stages of the parasite life cycle. We observed that gametocyte production, gamete fertilization, and the subsequent development of ookinetes and oocysts appeared unaffected by the absence of FabI, as judged by the similar numbers of oocysts that developed in *Anopheles stephensi* mosquitoes fed on mice infected with the *PbΔfabI*, *PbfabI*^{Rec}, or ANKA lines (data not shown). In two separate experiments, we observed no difference in the numbers of oocyst and salivary gland SPZs produced by these lines (data not shown).

To determine whether FabI plays a role in the infectivity of SPZs to the mammalian host, salivary gland SPZs were dissected and inoculated into the tail vein of C57BL/6 mice. This inbred strain of mouse was chosen as it is more susceptible than other inbred or outbred mouse strains to *P. berghei* SPZ infections (Scheller et al., 1994). Experiments were performed on three separate occasions and were highly reproducible. Intravenous injections of 1000 ANKA or *PbfabI*^{Rec} SPZs produced patent blood-stage infections that were microscopically detectable in 16/16 and 15/15 mice by day 5 (Table 2). In contrast, injection of 1000 *PbΔfabI* SPZs produced a blood-stage infection in only 5/16 mice, with the infected mice showing a delay in patency of 4 days. Increasing the *PbΔfabI* inoculum to 10,000 SPZs resulted in patent infections in 13/15 mice, with those mice again showing an average delay of 4 days compared to controls.

We also assayed the infectivity of SPZs delivered by mosquito bite to test for any defect in SPZ tissue traversal and migration from the dermis to the liver (Silvie et al., 2008b). Groups of 20 infected mosquitoes were allowed to feed on each mouse, with 5 mice tested per *P. berghei* line. Based on earlier studies, we estimate that each infected mosquito intradermally delivers ~120 SPZs (Medica and Sinnis, 2005), yielding an approximate inoculum of 2000 SPZs. Results showed that each mouse infected with ANKA or *PbfabI*^{Rec} parasites, as well as four of the five mice infected with *PbΔfabI* SPZs, developed a patent blood-stage infection. However, the latter group showed a 5 day delay (Table 2).

Taken together, the data demonstrate that *P. berghei* parasites lacking FabI produce SPZs that are highly attenuated in their infectivity to the mammalian host. We note that all “break-through” *PbΔfabI* asexual blood-stage infections became fulminant and lethal by days 20–29. This suggests that once *PbΔfabI* parasites developed into blood stages, they showed no loss of virulence compared to WT parasites. PCR analysis of break-through infections confirmed that they resulted from *PbΔfabI* parasites, and not from contamination with ANKA or *PbfabI*^{Rec} parasites (Figure S4F).

***PbΔfabI* SPZs Typically Fail to Produce Infectious Mature Liver-Stage Parasites**

To investigate the cause of this decreased infectivity of *PbΔfabI* SPZs, we first examined cell traversal and invasion of hepatocytes. The former occurs when SPZs transit through cells prior to initiating liver-stage development by forming a parasitophorous vacuole inside the invaded cell (Silvie et al., 2008b). In two independent experiments, rates of cell traversal were similar, with a mean of 9–13 dextran-positive (i.e., traversed) cells per field. *PbΔfabI* and *PbfabI*^{Rec} lines were also found to be equally competent for invasion, with 34%–38% success in invading Hepa 1-6 cells. We next assessed the maturing liver-stage parasites. At 24, 36, or 48 hr postinvasion, *PbΔfabI* and *PbfabI*^{Rec} parasites stained with antibodies specific for the

P. berghei cytosolic protein HSP70 (PB000817.02.0) showed equivalent numbers and developmental stages (data not shown). We also tested for *fabI* transcription in these stages. RT-PCR studies from infected Hepa 1-6 cells harvested 40 hr postinvasion revealed *pbfabI* mRNA transcripts in *PbfabI*^{Rec} but not *PbΔfabI* liver-stage parasites (Figure S4G). These results indicate that *fabI* is normally transcribed by liver-stage parasites; however, the lack of expression in *PbΔfabI* parasites did not affect SPZ cell traversal, invasion of hepatocytes, or the initial stages of intrahepatic development.

We proceeded to investigate later stages of liver-stage maturation using the HepG2 hepatoma cell line, which is able to support SPZ invasion and liver-stage development through to the production of merozoites that are infectious for RBCs. Immunofluorescence assays (IFAs) with mature hepatic stages were performed with antibodies that recognize the *P. berghei* parasite proteins Exp1 (PB000484.01.0) or MSP1 (PB000172.01.0). Exp1 is expressed throughout trophozoite development and schizogony and is exported into the PVM that separates the parasite from the host cell cytosol. In late liver stages, the Exp1-positive PVM is typically observed as a closed circular structure around the multiplying parasite nuclei (Sturm et al., 2006). In schizont stages, MSP1 is expressed and becomes integrated into the PPM. The PPM invaginates around pockets of parasite material during the cytomere stage and ultimately forms the membrane of individual merozoites (Sturm et al., 2008).

These antibodies revealed a striking difference between ANKA and *PbΔfabI* parasites very late in their liver-stage development. At 60 hr post SPZ invasion of HepG2 cells, 59% of the ANKA parasites were found to have developed into an advanced parasite stage marked by MSP1-positive PPM invaginations (Figures 4A and S5A). Many of these parasites were observed at the cytomere stage in which the PPM surrounded large groups of parasite nuclei (see row 2 in Figure S5A). The remaining 41% of parasites were MSP1 negative, indicating either delayed or aberrant development. In contrast, almost all *PbΔfabI* liver-stage parasites (99.5%) were negative for MSP1 staining, despite having initiated their development inside an Exp1-positive PVM (Figure 4A). In addition to the lack of MSP1 expression in *PbΔfabI* parasites, nuclear division was clearly impeded, as evidenced by the limited number of DAPI-positive parasite nuclei (Figure 4A). The very few MSP1-positive *PbΔfabI* liver-stage parasites that we did observe were restricted in size, with minimal PPM invaginations (Figures 4A and S5A). In support of this, at 60–65 hr postinvasion, we recorded no cytomere stage in over 3500 *PbΔfabI* liver-stage parasites, whereas cytomeres were observed in 266 ANKA parasites out of a total of 3366. At these late stages of parasite development, ANKA parasites began to degrade the PVM, as evidenced by their lack of the typical Exp1-positive closed circular structures seen in earlier stages (Figure S5B). This resulted in the generation of large clusters of MSP1-positive merozoites that filled the entire hepatocyte cytoplasm. Of these PVM-degraded, ANKA-infected cells, 87% contained MSP1-positive merozoites. The remaining 13% were MSP1 negative, suggesting that these had undergone aberrant development and had failed to produce viable merozoites (Figure S5B). In contrast, every *PbΔfabI* parasite that was found to have a nonintact PVM was MSP1-negative and was not producing mature merozoites (Figure S5B).

At the 65 hr time point, we also recorded the numbers of infected cells that had detached from the monolayer into the culture supernatant. These so-called “detached cells” harbor merozoites that have been released into the host cell cytoplasm following normal degradation of the PVM (Sturm et al., 2006). In three independent experiments, we did not observe a single detached cell with the *PbΔfabI* parasites. In contrast, detached cells numbered 210, 236, and 106 with ANKA parasites and 298, 136, and 103 with *PbfabI*^{Rec} parasites (Figure 4B). From these cultures, we also recorded the number of merosomes, i.e., the membrane-bound clusters of merozoites devoid of host nuclei that egress from the infected hepatocytes (Sturm et al., 2006, 2008). Merosomes were never observed in *PbΔfabI* liver-stage cultures in any of these three experiments. By comparison, ANKA parasites produced 69, 174, and 41 merosomes, while *PbfabI*^{Rec} parasites produced 77, 68, and 13 merosomes, respectively (Figure 4B). Similar results were obtained in three additional experiments that examined liver-stage parasites 70 hr postinvasion (data not shown), confirming a key role for FabI during the final maturation of the liver-stage schizont and the formation of merozoites.

While we never observed *PbΔfabI* merosomes, even after an extended culture period of 90 hr, we nevertheless recorded rare instances of MSP1-positive *PbΔfabI* merozoites. We also observed one instance of a cytomere stage at 70 hr postinvasion. The formation of these few merozoites and their passage into the blood stream might account for the *PbΔfabI* breakthrough blood-stage infections observed in vivo.

DISCUSSION

Here we report on the discovery that the FAS-II enzyme FabI plays a key role in the development of infectious liver-stage merozoites. Our study reveals a fundamental difference in how *Plasmodium* liver and asexual-stage parasites balance de novo synthesis and salvage of host factors to meet their FA requirements for intracellular parasite propagation. For asexual blood stages, our findings provide evidence against a recent report of an active FAS-II pathway (Suroliia and Suroliia, 2001) and instead support an alternate mechanism of FA modification that appears to act alongside a predominant import pathway.

The asymptomatic liver stage begins with SPZs productively infecting hepatocytes (Mikolajczak and Kappe, 2006; Prudencio et al., 2006). Following a prodigious phase of nuclear replication, parasites enter the cytomere stage, wherein nuclei distribute peripherally beneath the invaginating inner PPM. Later, the outer PVM disintegrates, releasing merozoites into the host cell cytoplasm. This process in vitro leads to cell detachment, followed by the destruction of host cell organelles, including the nucleus, and the formation of a host cell membrane-bounded merosome that is able to initiate a blood-stage infection (Sturm et al., 2006). Studies with *PbΔfabI* revealed a striking defect in liver-stage maturation. Whereas cell traversal, invasion, and initial development inside a parasitophorous vacuole proceeded normally, late *PbΔfabI* liver-stage parasites displayed a pronounced absence of the MSP1 parasite surface protein in the PPM. Furthermore, these parasites almost completely failed to develop to the cytomere stage, could not normally degrade their PVM, and exhibited an impaired development of merozoites. *PbΔfabI* parasites also

Cell Host & Microbe

A Key Role for FabI in Plasmodium Liver Stages

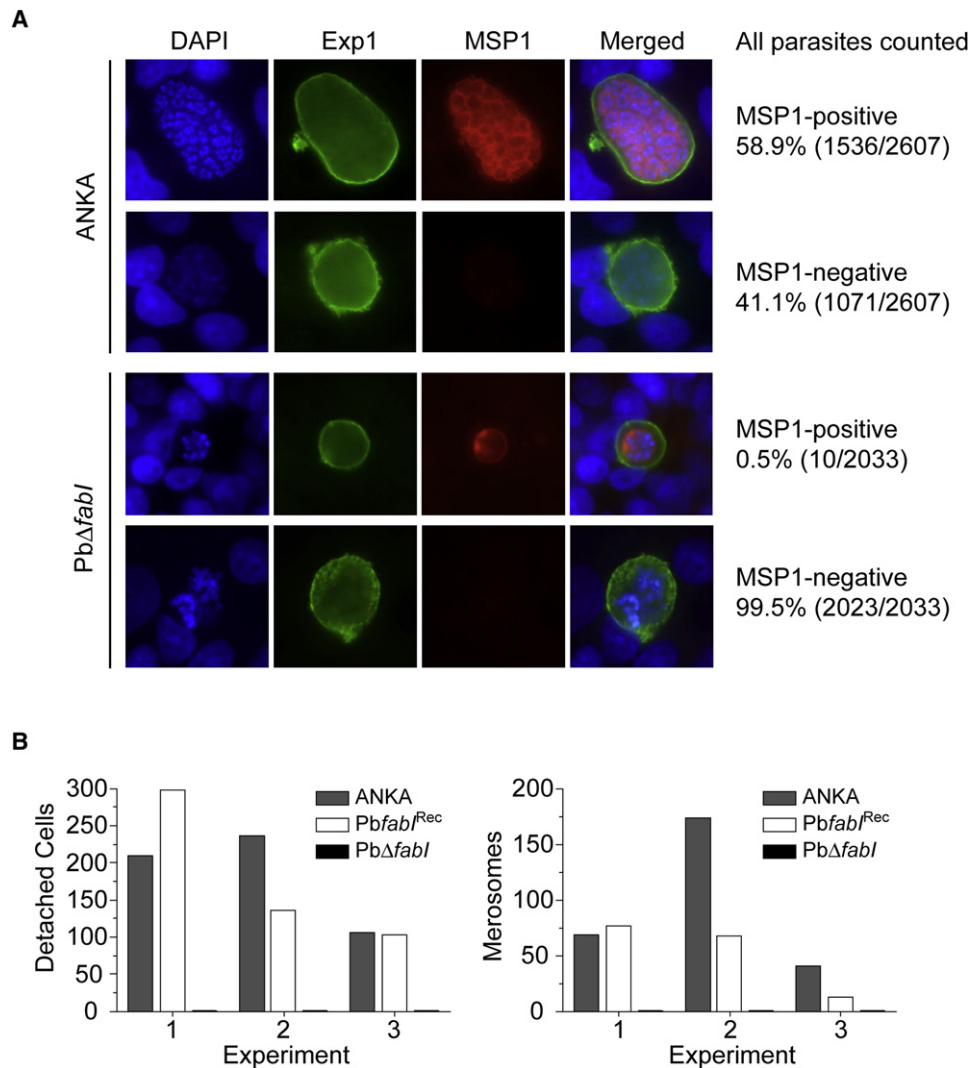


Figure 4. *P. berghei* $Pb\Delta fabI$ Parasites Exhibit a Strongly Impaired Merozoite Development and Fail to Form Detached Cells or Merozoites (A and B) IFA results of ANKA and $Pb\Delta fabI$ liver-stage parasites grown in vitro in HepG2 cells and examined 60 hr postinvasion. Parasites were stained with antibodies directed to Exp1 (green) or MSP1 (red), and DAPI (blue) was used to label the parasite and host cell nuclei. In (A), representative images of liver-stage parasites developing within an intact PVM are shown by Exp1 staining as a closed circle around the nuclei. Percentages and numbers of MSP1-positive or -negative parasites were collated from three independent experiments. Results show that most ANKA parasites (58.9%) developed normally and produced MSP1-positive merozoites, whereas very few $Pb\Delta fabI$ parasites (0.5%) were MSP1 positive. The upper panel shows a cytomere stage with typical membrane invaginations and arrangements of nuclei close to the PPM. In (B), for ANKA-, $Pb\Delta fabI$ -, and $Pb\Delta fabI^{Rec}$ -infected HepG2 cells, the numbers of detached cells and merozoites were quantified 65 hr postinvasion, in three independent experiments. These revealed a total absence of detached cells and merozoites in $Pb\Delta fabI$ liver-stage cultures. Additional representative images are presented in Figure S5.

displayed a near-total lack of cell detachment and merozoite formation (Figures 4 and S5). We posit that this developmental arrest explains the attenuated infectivity of $Pb\Delta fabI$ SPZs, as illustrated by their substantially delayed progression to blood-stage infection (Table 2). Residual infectivity was nevertheless observed, especially with the higher doses of 10^4 $Pb\Delta fabI$ SPZs that produced blood-stage infections in most mice. These “breakthrough” infections were fulminant and lethal, indicating that the few parasites that completed their liver-stage development were not attenuated for asexual blood-stage growth.

Dr. Stefan Kappe (Seattle Biomedical Research Institute) and colleagues have observed a similar phenotype of late liver-stage

arrest upon deletion of the FAS-II gene *fabB/F* in *P. yoelii* 17XNL. Their analysis of infected hepatocytes, obtained in BALB/c mice inoculated 44 hr prior with *fabB/F* knockout SPZs, revealed a lack of MSP1 staining and merozoite formation as well as a defect in PVM degradation (based on Hep17 expression) when compared to WT liver-stage parasites. In agreement with our observations, no attenuation was evident at other life-cycle stages for both *P. yoelii* *fabB/F* knockout parasites and a further knockout line that carried a deletion of *fabZ*. In contrast to $Pb\Delta fabI$ SPZs, the *P. yoelii* *fabB/F* knockout line failed to produce breakthrough asexual blood-stage infections, even with an inoculum as high as 100,000 salivary gland SPZs (S. Kappe, personal

communication). This might reflect differences in the virulence of the erythrocytic stages of *P. berghei* ANKA versus *P. yoelii* 17XNL. *P. berghei* ANKA parasites are known to rapidly produce a fulminant, lethal infection starting from low numbers of infected RBCs. In contrast, *P. yoelii* 17XNL infections are nonlethal and can be readily resolved by host immune responses. Alternatively, these species might differ in their dependence on FAS-II for successful liver-stage development.

Taken together, the FAS-II gene disruption data make a compelling case that de novo FA biosynthesis plays a key role in the successful production of the thousands of infectious merozoites produced per infected hepatocyte. While it is possible that FAS-II provides unique (i.e., unsalvageable) FAs, the detection of breakthrough infections with *PbΔfabI* suggests that its role is predominantly to augment levels of salvaged FAs to meet metabolic demands. Insights into the potential utilization of FAS-II products are provided by our investigations with *PbΔfabI*. These parasites revealed a pronounced deficit in their expression of MSP1, which is anchored to the parasite membrane via GPI moieties. These moieties are enriched in C_{16:0} (palmitic acid), C_{18:0} (stearic acid), and C_{18:1} (oleic acid) (Naik et al., 2000). How could these be produced by the liver-stage parasite? Biochemical studies with purified *P. falciparum* FAS-II enzymes provide evidence that this pathway produces predominantly C₁₀–C₁₄ FAs (Sharma et al., 2007). To modify these species into the saturated and unsaturated FAs found in GPI anchors would require the further action of elongases and desaturases (see below), whose activity in liver-stage parasites has been detected (Tarun et al., 2008). The inability of *PbΔfabI* liver-stage parasites to form cytomeres and normally degrade their PVM suggests that FAS-II products might also be incorporated into neutral glycerolipids, which have been implicated in intracellular vesicle trafficking, and membrane-resident phospholipids (Palacpac et al., 2004). Likewise, the failure of *PbΔfabI*-infected hepatocytes to form detached cells suggests that FAS-II products might contribute to parasite manipulation of the phospholipid composition of host cell membranes, a mechanism that appears to subvert immune recognition by liver phagocytes and that correlates with in vitro cell detachment (Sturm et al., 2006). This proposed central role of FAs in liver-stage biology agrees with recent transcriptome data showing that all four *P. yoelii* FAS-II genes are highly expressed in liver stages as compared to SPZs or asexual blood stages (Tarun et al., 2006). Those studies also revealed upregulation of members of the pyruvate dehydrogenase complex, whose production of acetyl-CoA primes the FAS-II pathway (Mazumdar and Striepen, 2007). These studies evoke the idea of targeting FAS-II enzymes for the development of a novel prophylactic antimalarial drug that clears liver-stage infections before they advance to the pathogenic erythrocytic stages.

In contrast to the phenotype of late liver-stage arrest observed upon disruption of the FAS-II pathway, other *Plasmodium* gene disruption studies have produced much earlier arrest. Dual disruption of the *P. yoelii* genes *p36* and *p52* (also termed *p36p*), individual knockouts of their orthologs in *P. berghei*, disruption of the *sap1/slap* gene in *P. yoelii* and *P. berghei*, and disruption of the *P. berghei* *uis4* or *uis3* genes all produced a developmental block within 24–48 hr postinvasion (Aly et al., 2008; Silvie et al., 2008a; references therein). Of the genetically attenuated SPZs,

those that did not cause breakthrough asexual blood-stage infections were found to elicit complete protective immunity against challenge with nonattenuated SPZs. We did not perform similar studies because of the finding that *PbΔfabI* SPZs could produce breakthrough parasitemias. Nevertheless, when compared to the other knockout lines, the delayed demise of *PbΔfabI* liver-stage parasites provides a greater window of antigen presentation, suggesting a potentially enhanced degree of immunogenicity (Jobe et al., 2007). Furthermore, given that the human parasite *P. falciparum* has a prodigious growth phase inside hepatocytes, on the order of 10,000–30,000 merozoites per infected cell as compared to 8,000–10,000 per hepatocyte for *P. berghei* and *P. yoelii* (Verhave and Meis, 1984), one might predict that the inability to produce sufficient levels of FAs through de novo synthesis could be severely detrimental for *P. falciparum*. Interestingly, the *P. berghei* PVM-resident protein UIS3 has been shown to bind L-FABP (liver-fatty acid binding protein), a key mediator of cellular uptake and transport of the FAs and lipid species that are abundant in hepatocytes (Furuhashi and Hotamisligil, 2008). This leads us to hypothesize that the disruption of liver-stage FA de novo synthesis and import might yield potent, genetically attenuated, pre-erythrocytic-stage vaccines in *Plasmodium* species, including *P. falciparum*.

Though the FAS-II pathway appears vitally important to liver-stage parasites, the analysis of our *PfΔfabI* and *PbΔfabI* lines argues against the earlier hypothesis that this pathway is required for asexual blood-stage propagation (Surolija et al., 2004). An alternative explanation of our data would be that another enoyl ACP-reductase might have compensated for the loss of FabI and thereby restored FAS-II functionality to the *ΔfabI* lines during their life cycle. Our bioinformatic search for alternate bacterial enoyl-ACP reductases (FabK, FabL, and FabV) (Massengo-Tiasse and Cronan, 2008) fail to identify any orthologs in *Plasmodium*, although this does not rule out their potential existence. Nonetheless, the blood and liver-stage phenotypes we observe with our *ΔfabI* lines have also been observed by Stefan Kappe and colleagues with transgenic *P. yoelii* parasites that lack *fabB/F* or *fabZ* (personal communication). Again, we have not found paralogs of these genes through bioinformatic searches of *Plasmodium* genomes. Our data, therefore, are consistent with a lack of requirement for the FAS-II pathway in asexual blood-stage parasites and support earlier evidence that these stages rely on salvage pathways for the bulk of their FA requirements (Vial and Ancelin, 1992).

In a remarkable body of work, Mi-Ichi et al. (Mi-Ichi et al., 2007, 2006) found that several combinations, including C_{16:0}/C_{18:0}/C_{18:2,n-6} or C_{16:0}/C_{18:1,n-9}/C_{18:2,n-6}, were sufficient to replace human serum or Albumax in malaria culture medium and permitted robust parasite growth for over 6 months. These various FAs are the predominant species present in human plasma and infected RBCs (Mi-Ichi et al., 2006). As per earlier reports (Krishnegowda and Gowda, 2003; Vial and Ancelin, 1992), these authors observed that salvaged FAs are predominantly incorporated into an unmodified form into parasite lipids. In addition, they observed FA modification via elongation or desaturation processes. This included the production of C_{16:0} and C_{18:0} from exogenous [¹⁴C]-C_{14:0} and [¹⁴C]-C_{16:0}, respectively, and desaturation of C_{18:0} to C_{18:1} (Mi-Ichi et al., 2006). In agreement with these findings, we also observed C₁₆ and C₁₈ FAs when incubating

Cell Host & Microbe

A Key Role for FabI in Plasmodium Liver Stages

P. falciparum parasites with [¹⁴C]-acetate, with no detectable difference between lines harboring or lacking FabI (Figures 3 and S2D). We also observed no such incorporation in control uninfected RBCs.

P. falciparum asexual blood-stage production of radiolabeled C₁₆ and C₁₈ FAs might involve elongases, three of which are encoded by this genome (Lee et al., 2007). The presence of four distinct elongases in the *P. berghei* genome might explain why this species was found to produce C₁₂–C₂₄ FAs (Figure 3). These ER-resident enzymes are responsible in mammals for producing very long chain FAs (≥C₁₈) and, in trypanosomes, producing C₁₀–C₁₈ FAs (Jakobsson et al., 2006; Lee et al., 2006). *P. falciparum* asexual blood stages are also capable of modifying FAs via desaturation of C_{16:0} and C_{18:0} at the n-9 position, presumably via their Δ⁹ desaturase (PFE0555w) (Mi-Ichi et al., 2006). Another crucial step in the intraerythrocytic modification of imported host FAs may involve acyl-CoA synthetase enzymes, which activate acyl chains for entry into FA synthesis, desaturation, and elongation pathways. Members of this gene family are present in 4–12 copies in *Plasmodium* species, and biochemical assays have shown 20-fold higher acyl-CoA synthetase activity in infected versus uninfected RBCs (Bethke et al., 2006; Vial and Ancelin, 1992).

FabI has been extensively studied as a candidate drug target for asexual blood-stage parasites. Yet our data now argue against the therapeutic potential of this target, and indeed the entire FAS-II pathway, during erythrocytic infection. These data imply that, contrary to earlier suppositions (Ralph et al., 2004; Surolia et al., 2004), asexual blood-stage parasites do not require FAS-II activity in the apicoplast. Focusing on FabI, our transgene overexpression and gene disruption studies demonstrate that this is not the target of the antimalarial activity of triclosan (Figures 2, S1, S2, and S4), despite an earlier report of its inhibition of FA biosynthesis in asexual blood-stage parasites and its high affinity for purified enzyme (Perozzo et al., 2002; Surolia and Surolia, 2001). These data agree with studies of *Trypanosoma brucei* parasites that discount FabI as the target of triclosan and have proposed nonspecific membrane perturbation as an alternate mode of action (Lee et al., 2007). Our studies nevertheless find that triclosan has activity against *Plasmodium* asexual blood-stage parasites and is efficacious in vivo (Figure 1), albeit at concentrations substantially higher than previously reported (Surolia and Surolia, 2001). Further studies are required to elucidate how triclosan acts upon asexual blood-stage parasites. In these stages, it is now clear that exogenous FAs are essential. We propose that therapeutic strategies to interfere with FA processes in asexual blood-stage parasites should focus on import and subsequent modification, presumably mediated by elongases, the Δ⁹ desaturase, and acyl CoA-synthetases. This contrasts with liver-stage parasites where interference with FAS-II offers novel perspectives for prophylactic intervention.

EXPERIMENTAL PROCEDURES

Parasite Propagation

P. falciparum lines (Table 1) and *P. berghei* ANKA parasites were propagated as described in the Supplemental Data. All experiments involving rodents were conducted in fully accredited animal facilities and were approved by the Institutional Animal Care and Use Committees of Columbia University, the Albert Einstein College of Medicine, the New York University Medical Center, the University of Miami, and the Bernhard Nocht Institute for Tropical Medicine.

Parasite In Vitro and In Vivo Drug Susceptibility Assays

The synthesis of triclosan analogs has been previously described (Freundlich et al., 2007; references therein). For enzyme inhibition assays, the reaction mixtures contained 50 nM PfFabI, 400 μM NADH, and 40 μM NAD⁺, and were initiated with 300 μM butyryl-CoA. Inhibition of PfFabI-mediated butyryl-CoA reduction was assessed spectrophotometrically by measuring the oxidation of NADH to NAD⁺ at 340 nm (Freundlich et al., 2007). EC₅₀ values represent the analog concentration that inhibited maximal PfFabI activity by 50%. Inhibition of *P. falciparum* in vitro or *P. berghei* ex vivo parasite growth was measured using [³H]hypoxanthine assays, and the IC₅₀ values were calculated using linear regression (see Supplemental Data). All compounds were tested in duplicate on at least two separate occasions. For in vivo efficacy studies, CD-1 mice were infected intraperitoneally on day 0 with 5 × 10⁴ *P. berghei* asexual blood-stage parasites. Triclosan (Vita-Pharm; Valhalla, NY) was administered on days 3, 4, and 5 after infection as two divided doses daily, spaced 6 hr apart, delivered either PO or SC. Parasitemias were determined from Giemsa-stained smears of tail blood, collected on day 6 and twice a week thereafter until day 31 (see Supplemental Data).

Plasmid Constructs, Parasite Transfections, Nucleic Acid and Protein Analyses, Immunofluorescence Assays, and Structural Elucidation of PbFabI

These are detailed in the Supplemental Data. Primers are listed in Table S2, and transfection plasmids and parasite lines are listed in Table 1.

FA Extraction and HPLC Analysis

P. falciparum- or *P. berghei*-infected RBCs were labeled with [¹⁴C]-acetate (10 μCi/ml) for 6 hr or 24 hr, respectively, at 37°C. Parasite pellets were obtained by saponin lysis and washed twice to remove host cell components, and the FAs were analyzed by reversed-phase HPLC (see Supplemental Data).

P. berghei Infection of Mosquitoes, Sporozoite Invasion and Cell Traversal Assays, and Analysis of Liver-Stage Development

Experimental conditions are detailed in the Supplemental Data.

Determination of *P. berghei* Prepatent Periods in Mice

To determine the in vivo infectivity of mutant and control parasite lines, naive C57BL/6 mice were injected intravenously with 1,000 or 10,000 *P. berghei* salivary gland SPZs or subjected to the bite of 20 infected mosquitoes that were allowed to probe for 6 min. Asexual blood-stage infection was determined by Giemsa-stained blood smears prepared on days 3–28 after SPZ inoculation.

SUPPLEMENTAL DATA

The Supplemental Data includes Supplemental Experimental Procedures, Supplemental References, five figures, and two tables and can be found online at [http://www.cell.com/cellhostandmicrobe/supplemental/S1931-3128\(08\)00368-5](http://www.cell.com/cellhostandmicrobe/supplemental/S1931-3128(08)00368-5).

ACKNOWLEDGMENTS

We thank Drs. Geoff McFadden and Anthony Holder for the *P. falciparum* ACP and *P. yoelii* MSP1 antibodies and the Fidock lab members for helpful discussions. PFERD2 rabbit antiserum (MRA-1) was obtained through the MR4, deposited by John Adams. This work was supported by the National Institutes of Health (P01 AI060342, J.C.S., D.A.F., and W.R.J.; and R01 AI056840, P.S.), the Medicines for Malaria Venture (D.A.F., J.C.S., W.R.J., and D.A.J.), the Robert A. Welch Foundation (J.C.S.), the Deutsche Forschungsgesellschaft (DFG) (4497/1-2, V.H.), the Ministère de l'Éducation Nationale de la Recherche et des Technologies (P.G.), and the Centre National de la Recherche Scientifique (L.K.). The authors all declare no conflict of interests.

Received: September 24, 2008

Revised: November 3, 2008

Accepted: November 5, 2008

Published: December 10, 2008

REFERENCES

- Aly, A.S., Mikolajczak, S.A., Rivera, H.S., Camargo, N., Jacobs-Lorena, V., Labaied, M., Coppens, I., and Kappe, S.H. (2008). Targeted deletion of SAP1 abolishes the expression of infectivity factors necessary for successful malaria parasite liver infection. *Mol. Microbiol.* 69, 152–163.
- Amino, R., Giovannini, D., Thiberge, S., Gueirard, P., Boisson, B., Dubremetz, J.F., Prevost, M.C., Ishino, T., Yuda, M., and Menard, R. (2008). Host cell traversal is important for progression of the malaria parasite through the dermis to the liver. *Cell Host Microbe* 3, 88–96.
- Bethke, L.L., Zilversmit, M., Nielsen, K., Daily, J., Volkman, S.K., Ndiaye, D., Lozovsky, E.R., Hartl, D.L., and Wirth, D.F. (2006). Duplication, gene conversion, and genetic diversity in the species-specific acyl-CoA synthetase gene family of *Plasmodium falciparum*. *Mol. Biochem. Parasitol.* 150, 10–24.
- Freundlich, J.S., Wang, F., Tsai, H.C., Kuo, M., Shieh, H.M., Anderson, J.W., Nkrumah, L.J., Valderramos, J.C., Yu, M., Kumar, T.R., et al. (2007). X-ray structural analysis of *Plasmodium falciparum* enoyl acyl carrier protein reductase as a pathway towards the optimization of triclosan antimalarial efficacy. *J. Biol. Chem.* 282, 25436–25444.
- Furuhashi, M., and Hotamisligil, G.S. (2008). Fatty acid-binding proteins: role in metabolic diseases and potential as drug targets. *Nat. Rev. Drug Discov.* 7, 489–503.
- Gilson, P.R., Nebl, T., Vukcevic, D., Moritz, R.L., Sargeant, T., Speed, T.P., Schofield, L., and Crabb, B.S. (2006). Identification and stoichiometry of glycosylphosphatidylinositol-anchored membrane proteins of the human malaria parasite *Plasmodium falciparum*. *Mol. Cell. Proteomics* 5, 1286–1299.
- Greenwood, B.M., Fidock, D.A., Kyle, D.E., Kappe, S.H., Alonso, P.L., Collins, F.H., and Duffy, P.E. (2008). Malaria: progress, perils, and prospects for eradication. *J. Clin. Invest.* 118, 1266–1276.
- Jakobsson, A., Westerberg, R., and Jacobsson, A. (2006). Fatty acid elongases in mammals: their regulation and roles in metabolism. *Prog. Lipid Res.* 45, 237–249.
- Jobe, O., Lumsden, J., Mueller, A.K., Williams, J., Silva-Rivera, H., Kappe, S.H., Schwenk, R.J., Matuschewski, K., and Krzych, U. (2007). Genetically attenuated *Plasmodium berghei* liver stages induce sterile protracted protection that is mediated by major histocompatibility complex Class I-dependent interferon-gamma-producing CD8+ T cells. *J. Infect. Dis.* 196, 599–607.
- Kapoor, M., Gopalakrishnapai, J., Surolia, N., and Surolia, A. (2004). Mutational analysis of the triclosan-binding region of enoyl-ACP (acyl-carrier protein) reductase from *Plasmodium falciparum*. *Biochem. J.* 381, 735–741.
- Krishnegowda, G., and Gowda, D.C. (2003). Intraerythrocytic *Plasmodium falciparum* incorporates extraneous fatty acids to its lipids without any structural modification. *Mol. Biochem. Parasitol.* 132, 55–58.
- Lee, S.H., Stephens, J.L., Paul, K.S., and Englund, P.T. (2006). Fatty acid synthesis by elongases in trypanosomes. *Cell* 126, 691–699.
- Lee, S.H., Stephens, J.L., and Englund, P.T. (2007). A fatty-acid synthesis mechanism specialized for parasitism. *Nat. Rev. Microbiol.* 5, 287–297.
- Massengo-Tiasse, R.P., and Cronan, J.E. (2008). *Vibrio cholerae* FabV defines a new class of enoyl-acyl carrier protein reductase. *J. Biol. Chem.* 283, 1308–1316.
- Mazumdar, J., and Striepen, B. (2007). Make it or take it: fatty acid metabolism of apicomplexan parasites. *Eukaryot Cell* 6, 1727–1735.
- Medica, D.L., and Sinnis, P. (2005). Quantitative dynamics of *Plasmodium yoelii* sporozoite transmission by infected anopheline mosquitoes. *Infect. Immun.* 73, 4363–4369.
- Mi-ichi, F., Kita, K., and Mitamura, T. (2006). Intraerythrocytic *Plasmodium falciparum* utilize a broad range of serum-derived fatty acids with limited modification for their growth. *Parasitology* 133, 399–410.
- Mi-ichi, F., Kano, S., and Mitamura, T. (2007). Oleic acid is indispensable for intraerythrocytic proliferation of *Plasmodium falciparum*. *Parasitology* 134, 1671–1677.
- Mikolajczak, S.A., and Kappe, S.H. (2006). A clash to conquer: the malaria parasite liver infection. *Mol. Microbiol.* 62, 1499–1506.
- Muralidharan, J., Suguna, K., Surolia, A., and Surolia, N. (2003). Exploring the interaction energies for the binding of hydroxydiphenyl ethers to enoyl-acyl carrier protein reductases. *J. Biomol. Struct. Dyn.* 20, 589–594.
- Naik, R.S., Branch, O.H., Woods, A.S., Vijaykumar, M., Perkins, D.J., Nahlen, B.L., Lal, A.A., Cotter, R.J., Costello, C.E., Ockenhouse, C.F., et al. (2000). Glycosylphosphatidylinositol anchors of *Plasmodium falciparum*: molecular characterization and naturally elicited antibody response that may provide immunity to malaria pathogenesis. *J. Exp. Med.* 192, 1563–1576.
- Nkrumah, L.J., Muhle, R.A., Moura, P.A., Ghosh, P., Hatfull, G.F., Jacobs, W.R., Jr., and Fidock, D.A. (2006). Efficient site-specific integration in *Plasmodium falciparum* chromosomes mediated by mycobacteriophage Bxb1 integrase. *Nat. Methods* 3, 615–621.
- Palapac, N.M., Hiramane, Y., Mi-ichi, F., Torii, M., Kita, K., Hiramatsu, R., Horii, T., and Mitamura, T. (2004). Developmental-stage-specific triacylglycerol biosynthesis, degradation and trafficking as lipid bodies in *Plasmodium falciparum*-infected erythrocytes. *J. Cell Sci.* 117, 1469–1480.
- Perozzo, R., Kuo, M., bir Singh Sidhu, A., Valiyaveetil, J.T., Bittman, R., Jacobs, W.R., Jr., Fidock, D.A., and Sacchetti, J.C. (2002). Structural elucidation of the specificity of the antibacterial agent triclosan for malarial enoyl ACP reductase. *J. Biol. Chem.* 277, 13106–13114.
- Prudencio, M., Rodriguez, A., and Mota, M.M. (2006). The silent path to thousands of merozoites: the *Plasmodium* liver stage. *Nat. Rev. Microbiol.* 4, 849–856.
- Ralph, S.A., van Dooren, G.G., Waller, R.F., Crawford, M.J., Fraunholz, M.J., Foth, B.J., Tonkin, C.J., Roos, D.S., and McFadden, G.I. (2004). Tropical infectious diseases: metabolic maps and functions of the *Plasmodium falciparum* apicoplast. *Nat. Rev. Microbiol.* 2, 203–216.
- Scheller, L.F., Wirtz, R.A., and Azad, A.F. (1994). Susceptibility of different strains of mice to hepatic infection with *Plasmodium berghei*. *Infect. Immun.* 62, 4844–4847.
- Sharma, S., Sharma, S.K., Modak, R., Karmodiya, K., Surolia, N., and Surolia, A. (2007). Mass spectrometry-based systems approach for identification of inhibitors of *Plasmodium falciparum* fatty acid synthase. *Antimicrob. Agents Chemother.* 51, 2552–2558.
- Silvie, O., Goetz, K., and Matuschewski, K. (2008a). A sporozoite asparagine-rich protein controls initiation of *Plasmodium* liver stage development. *PLoS Pathog.* 4, e1000086.
- Silvie, O., Mota, M.M., Matuschewski, K., and Prudencio, M. (2008b). Interactions of the malaria parasite and its mammalian host. *Curr. Opin. Microbiol.* 11, 352–359.
- Sturm, A., Amino, R., van de Sand, C., Regen, T., Retzlaff, S., Renneberg, A., Krueger, A., Pollok, J.M., Menard, R., and Heussler, V.T. (2006). Manipulation of host hepatocytes by the malaria parasite for delivery into liver sinusoids. *Science* 313, 1287–1290.
- Sturm, A., Retzlaff, S., Franke-Fayard, B., Graewe, S., Bolte, S., Roppenser, B., Apfelfbacher, M., Janse, C.J., and Heussler, V.T. (2008). Alteration of the parasite membrane and the parasitophorous vacuole membrane during exo-erythrocytic development of malaria parasites. *Protist*, in press.
- Surolia, N., and Surolia, A. (2001). Triclosan offers protection against blood stages of malaria by inhibiting enoyl-ACP reductase of *Plasmodium falciparum*. *Nat. Med.* 7, 167–173.
- Surolia, A., Ramya, T.N., Ramya, V., and Surolia, N. (2004). ‘FAS’ inhibition of malaria. *Biochem. J.* 383, 401–412.
- Tarun, A.S., Baer, K., Dumpit, R.F., Gray, S., Lejarcegui, N., Frevert, U., and Kappe, S.H. (2006). Quantitative isolation and *in vivo* imaging of malaria parasite liver stages. *Int. J. Parasitol.* 36, 1283–1293.
- Tarun, A.S., Peng, X., Dumpit, R.F., Ogata, Y., Silva-Rivera, H., Camargo, N., Daly, T.M., Bergman, L.W., and Kappe, S.H. (2008). A combined transcriptome and proteome survey of malaria parasite liver stages. *Proc. Natl. Acad. Sci. USA* 105, 305–310.
- Verhave, J.P., and Meis, J.F. (1984). The biology of tissue forms and other asexual stages in mammalian plasmodia. *Experientia* 40, 1317–1329.
- Vial, H.J., and Ancelin, M.L. (1992). Malarial lipids. An overview. *Subcell. Biochem.* 18, 259–306.
- Zhang, Y.M., White, S.W., and Rock, C.O. (2006). Inhibiting bacterial fatty acid synthesis. *J. Biol. Chem.* 281, 17541–17544.